Tectonophysics, 130 (1986) 369–383
Elsevier Science Publishers B.V., Amsterdam – Printed in The Netherlands

INTEGRATION OF GEODETIC AND GEOTECHNICAL DEFORMATION SURVEYS IN THE GEOSCIENCES

ADAM CHRZANOWSKI, YONGQI CHEN *, PABLO ROMERO and JAMES M. SECORD

Department of Surveying Engineering, University of New Brunswick, P.O. Box 4400, Fredericton, N.B. E3B 5A3 (Canada)

(Accepted March 18, 1986)

ABSTRACT

Chrzanowski, A., Chen, Y.Q., Romero, P. and Secord, J.M., 1986. Integration of geodetic and geotechnical deformation surveys in the geosciences. In: H.G. Henneberg (Editor), Recent Crustal Movements, 1985. *Tectonophysics*, 130: 369–383.

Ground movement studies can utilize information from conventional geodetic surveying, photogrammetry, and geotechnical measurements of strain, tilt, etc. Each method alone cannot yield a complete picture of the deformation. However, each is complemented by the others. Hence, their integration in a simultaneous analysis in space and in time is advocated. An integrated analysis is readily accommodated by a generalized method of deformation analysis devised by the authors. Any number of measurements of any type can be considered in any fashion of modelling with full statistical assessment of the modelling and of derived characteristics. Such an integration is illustrated using data from a coal mining area in rugged mountainous terrain of western Canada. Conventional terrestrial geodetic methods connected 15 stations. Displacements from an additional 29 points were obtained from aerial photogrammetry. Biaxial tiltmeters continuously measured ground tilts at 3 stations. A surface of subsidence for the whole area was modelled with the graphical depiction in three dimensions.

1. INTRODUCTION

Monitoring surveys in the geosciences, for purposes such as investigations of tectonic movements, landslides, or natural or man-induced ground subsidence, can be categorized into three main groups according to the methodology and instrumentation used: geodetic surveying methods; photogrammetric surveys; and geotechnical measurements (using strainmeters, extensometers, tiltmeters, etc.).

Geodetic surveys offer high accuracy in the relative positioning of discrete monitoring points and give a global picture of the status of deformation. However,

* On leave from the Wuhan Technical University of Surveying and Mapping, Wuhan, P.R. of China.

0040-1951/86/$03.50

they are slow and their adaptation to continuous and automatic monitoring is difficult and expensive.

Photogrammetric surveys provide an instant capture of the deformation status of the whole object of interest, including inaccessible areas, and the field work is relatively light. But their accuracy is not always sufficient.

Geotechnical surveys supply highly accurate information regarding deformation and are easily adaptable for continuous, fully automatic and telemetric data acquisition. In comparison with the two other methods, they are independent of environmental conditions such as snow coverage or poor visibility. However, they provide only local information at discrete points.

Each of the above methods, if used separately, may lead to physical misinterpretation of the actual deformation. For example, change in the distances in a geodetic network in a seismically active area may be prematurely interpreted as strain accumulation, while in reality the observed changes could be produced just by rigid body dislocation of the geodetic points due to discontinuities in the deformable object. In this case, the addition of local strain measurements could help in arriving at a proper deformation model.

From the above, one can clearly see that each of the three methods complements the other two. Therefore, an integration of the different methods is recommended.

In practice, one could find many monitoring projects where the data from geotechnical and geodetic measurements have been collected and analysed separately by different specialists without any attempt to integrate or, at least, to exchange the information for a better understanding of the deformation mechanism.

The authors have developed a generalized approach (Chen, 1983; Chrzanowski et al., 1983) to the deformation analysis in which any type of observations measured in several campaigns can be analysed simultaneously in space and time. A summary of the approach is given below together with an example of its application to a ground subsidence study in which geodetic, photogrammetric, and geotechnical measurements have been integrated in a simultaneous geometrical analysis.

2. BASIC PRINCIPLE OF THE GENERALIZED APPROACH

The deformation of a body is fully described in three dimensions if nine deformation parameters, i.e., six strain and three differential rotation components, can be determined at each point. In addition, components of relative rigid body motion between blocks should also be determined if discontinuities exist in the body. The above deformation parameters can be easily calculated if a displacement function $\boldsymbol{d}(x, y, z; t-t_0)$ is known (e.g., Sokolnikoff, 1956). Since, in practice, deformation surveys are made only at discrete points, displacement function must be approximated through some selected model which fits into the observation data in the best possible way.

The displacement function can be written in matrix notation as:

$$\boldsymbol{d}(x, y, z; t - t_0) = \begin{pmatrix} u(x, y, z; t - t_0) \\ v(x, y, z; t - t_0) \\ w(x, y, z; t - t_0) \end{pmatrix} = \boldsymbol{Bc} \tag{1}$$

where u, v, w are the components of the displacement in the x, y, z directions, respectively, $\boldsymbol{B}$ is the deformation matrix with its elements being functions of the position of the observation points and of time, and $\boldsymbol{c}$ is the vector of unknown coefficients. A vector $\Delta \boldsymbol{l}$ of changes in any type of observations or quasi-observations, for instance the coordinates derived from photogrammetric surveys, can be expressed in terms of the displacement function as:

$$\Delta \boldsymbol{l} = \boldsymbol{ABc} = \tilde{\boldsymbol{B}}\boldsymbol{c} \tag{2}$$

where $\boldsymbol{A}$ is the transformation matrix (or configuration matrix) relating the observations to the displacements. In the case of the observations being changes in coordinates (displacements) of the observed points, the matrix $\boldsymbol{A}$ becomes the identity matrix. The functional relationship between different types of observables and coefficient vector $\boldsymbol{c}$ is given in Appendix I.

If redundant observations are made, the elements of the unknown vector $\boldsymbol{c}$ are estimated through the least-squares approximation:

$$\hat{\boldsymbol{c}} = \left(\tilde{\boldsymbol{B}}^{\mathrm{T}} \boldsymbol{P}_{\Delta l} \tilde{\boldsymbol{B}} \right)^{-1} \tilde{\boldsymbol{B}}^{\mathrm{T}} \boldsymbol{P}_{\Delta l} \, \Delta \boldsymbol{l} \tag{3}$$

and have the covariance matrix

$$\boldsymbol{C}_{\hat{c}} = \sigma_0^2 \left(\tilde{\boldsymbol{B}}^{\mathrm{T}} \boldsymbol{P}_{\Delta l} \tilde{\boldsymbol{B}} \right)^{-1} \tag{4}$$

where $\boldsymbol{P}_{\Delta l}$ is the weight matrix for $\Delta \boldsymbol{l}$, and σ_0^2 is the variance factor.

In a more general case, when a simultaneous multi-epoch analysis of the observables $\boldsymbol{y}_i$ ($i = 1, 2, \ldots, k$ epochs) is performed, a general solution to the vector $\boldsymbol{c}$ has been elaborated in Chen (1983), and reads as:

$$\hat{\boldsymbol{c}} = \left[\sum_2^k \tilde{\boldsymbol{B}}_i^{\mathrm{T}} \boldsymbol{P}_i \tilde{\boldsymbol{B}}_i - \sum_2^k \tilde{\boldsymbol{B}}_i^{\mathrm{T}} \boldsymbol{P}_i \left(\sum_1^k \boldsymbol{P}_i \right)^{-1} \sum_2^k \boldsymbol{P}_i \tilde{\boldsymbol{B}}_i \right]^{-1} \cdot \left[\sum_2^k \tilde{\boldsymbol{B}}_i^{\mathrm{T}} \boldsymbol{P}_i \boldsymbol{y}_i - \sum_2^k \tilde{\boldsymbol{B}}_i^{\mathrm{T}} \boldsymbol{P}_i \left(\sum_1^k \boldsymbol{P}_i \right)^{-1} \sum_1^k \boldsymbol{P}_i \boldsymbol{y}_i \right] \tag{5}$$

where $\boldsymbol{P}_i$ is the weight matrix of observations in epoch i.

The above solution takes care of possible datum and configuration defects in the monitoring network when quasi-observations are involved.

It can be shown that the solution (3) is a special case of the general solution (5) when only two epochs are considered.

The generalized approach is applicable to any type of geometrical analysis, both in space and in time, including the detection of an unstable area and the determination of strain components and relative rigid body motion within a deformed object. It allows utilization of different types of surveying data and geotechnical measurements. In practical application, the approach consists of three basic processes: identification of deformation models; estimation of the deformation parameters; diagnostic checking of the models and the final selection of the "best" model.

The analysis procedures using the approach can be summarized in the following steps:

Step 1. Assessment of the observations using the minimum norm quadratic unbiased estimation (MINQUE) principle to obtain the variances of observations and possible correlations of the observations within one epoch or between epochs, if the a priori values are not available.

Step 2. Separate adjustment of each epoch of geodetic or photogrammetric observations, if such are available, for detection of outliers and systematic errors. If correlations of the observations between epochs are not negligible, then simultaneous adjustment of multiple epochs of observations is required.

Steps 1 and 2 overlap because the existence of outliers and systematic errors will influence the estimated variances and covariances and the adopted variances and covariances of the observations will affect outlier detection.

Step 3. Comparison of pairs of epochs; selection of deformation models based on a priori considerations and trend analysis from the displacement pattern, if such is available from the observations. If a monitoring network suffers from datum defects, the method of iterative weighted projection (Chen, 1983) is used to yield the "best" picture of the displacement pattern. Examples of typical deformation models are given in Appendix II for illustration.

Step 4. Estimation of the coefficients of deformation models and their covariances using all available information.

Step 5. Global test on the deformation model; testing groups of coefficients or an individual one for significance.

The above three steps should be considered as an iterative three-step procedure, so they necessarily overlap.

Step 6. Simultaneous estimation of the coefficients of the deformation model in space and in time if the analysis of pairs of epochs of observations suggests that it is worth doing.

This simultaneous estimation must be performed if the observations are scattered in time. The iterative three-step procedure is still valid. The possible deformation models can be selected either based on a priori considerations or by plotting the observations versus time for trend analysis.

Step 7. Comparison of the models and choice of the "best" model. Since more than one of several possible models could fit the data reasonably well, the "best" model is selected according to the criteria: (a) the model passes the global statistical test at an acceptable probability; (b) if more than one model passes the global test, then the model with the fewest significant coefficients is selected; (c) if the two above criteria cannot be satisfied, then the rationale based on physical grounds and minimal error of fit is used.

Step 8. Calculation of the desired deformation characteristics and their accuracies from the parameters of the "best" model.

Step 9. Graphical display of the deformation model.

A detailed description of the above steps can be found in Secord (1984).

3. APPLICATION OF THE GENERALIZED APPROACH TO A SUBSIDENCE STUDY

The generalized approach has been applied in an integrated analysis of survey data collected in rugged mountainous terrain of western Canada over an underground coal-mining operation which is described in Fisekci and Chrzanowski (1981). The purpose of the surveys was to monitor ground movements caused by coal extraction. Three types of observations in three dimensions were used in the integrated analysis of the ground subsidence: changes in coordinates of 15 points determined by terrestrial geodetic methods, changes in coordinates of 29 points calculated from aerial photogrammetric surveys, and changes in ground tilts at three stations obtained from remotely controlled bi-axial tiltmeters (Chrzanowski and Fisekci, 1982). Figure 1 shows the locations of the points with respect to the extracted coal panel. The geodetic positioning surveys, which were performed by the polar method from stations located outside the subsidence area, could be performed only during the short summer periods when the sighted points were not covered by snow. Similarly restricted were the photogrammetric surveys which are described with more detail in Armenakis and Faig (1982).

The tiltmeter observations were performed continuously with a telemetric data acquisition system which was developed at the University of New Brunswick (Chrzanowski et al., 1980).

For the illustration of the application of the generalized approach, only two campaigns (two epochs) of geodetic and photogrammetric observations (summers of 1980 and 1982) have been analysed, including the tiltmeter data extracted from the continuous record (Fig. 2) for these two epochs only. Approximate coordinates of all the survey points (including the tiltmeter stations) and the observed displacements (quasi-observables) and tilts, with their corresponding standard deviations in metres and seconds of arc, are listed in Table 1.

The following observation equations were used in the least-squares fitting of selected deformation models (displacement functions) into the observations:

For geodetic and photogrammetric displacements at point i:

$$\mathrm{d}x_i = u(x_i,\ y_i) \tag{6a}$$

$$\mathrm{d}y_i = v(x_i,\ y_i) \tag{6b}$$

$$\mathrm{d}z_i = w(x_i,\ y_i) \tag{6c}$$

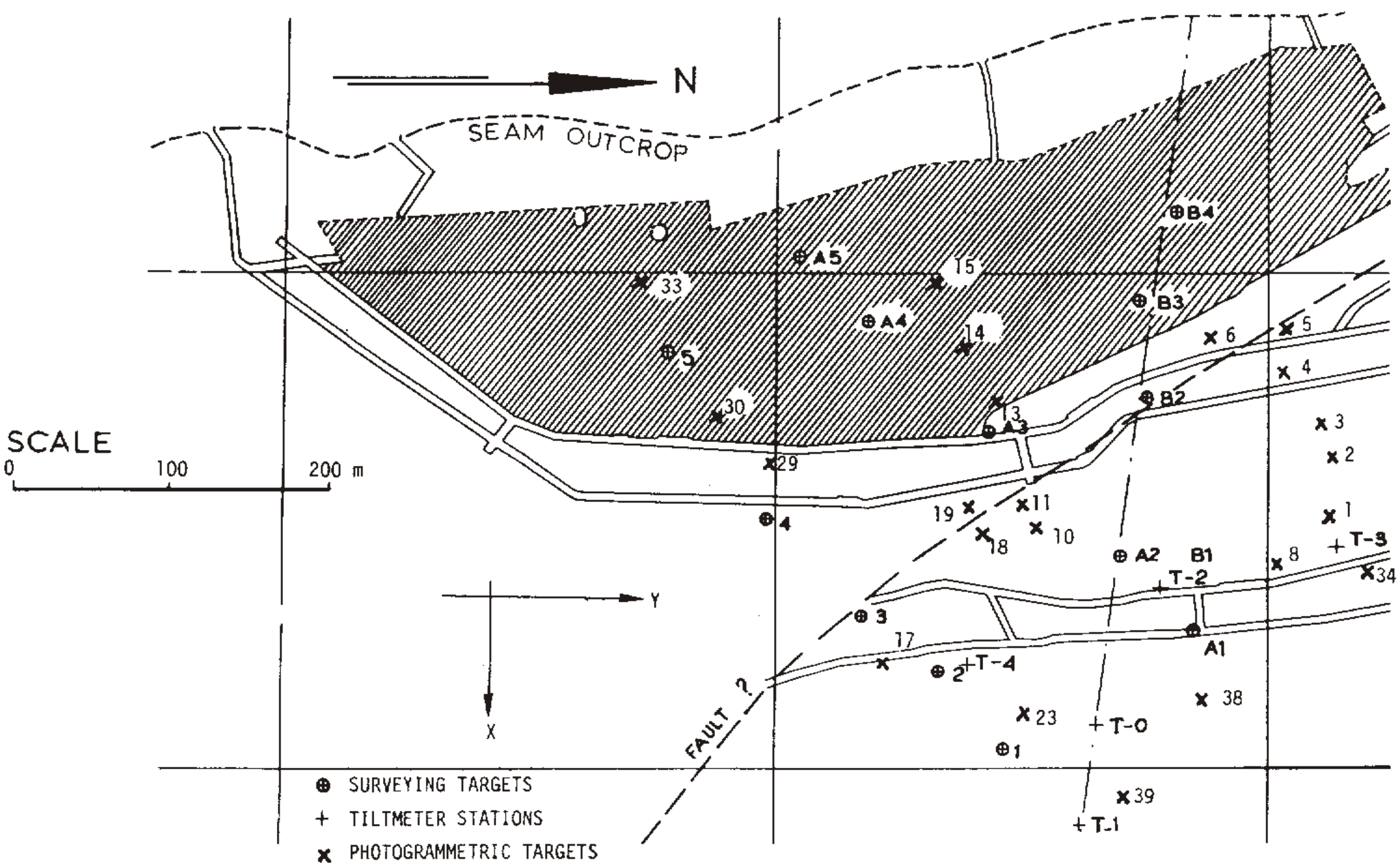

Fig. 1. Locations of the monitoring stations.

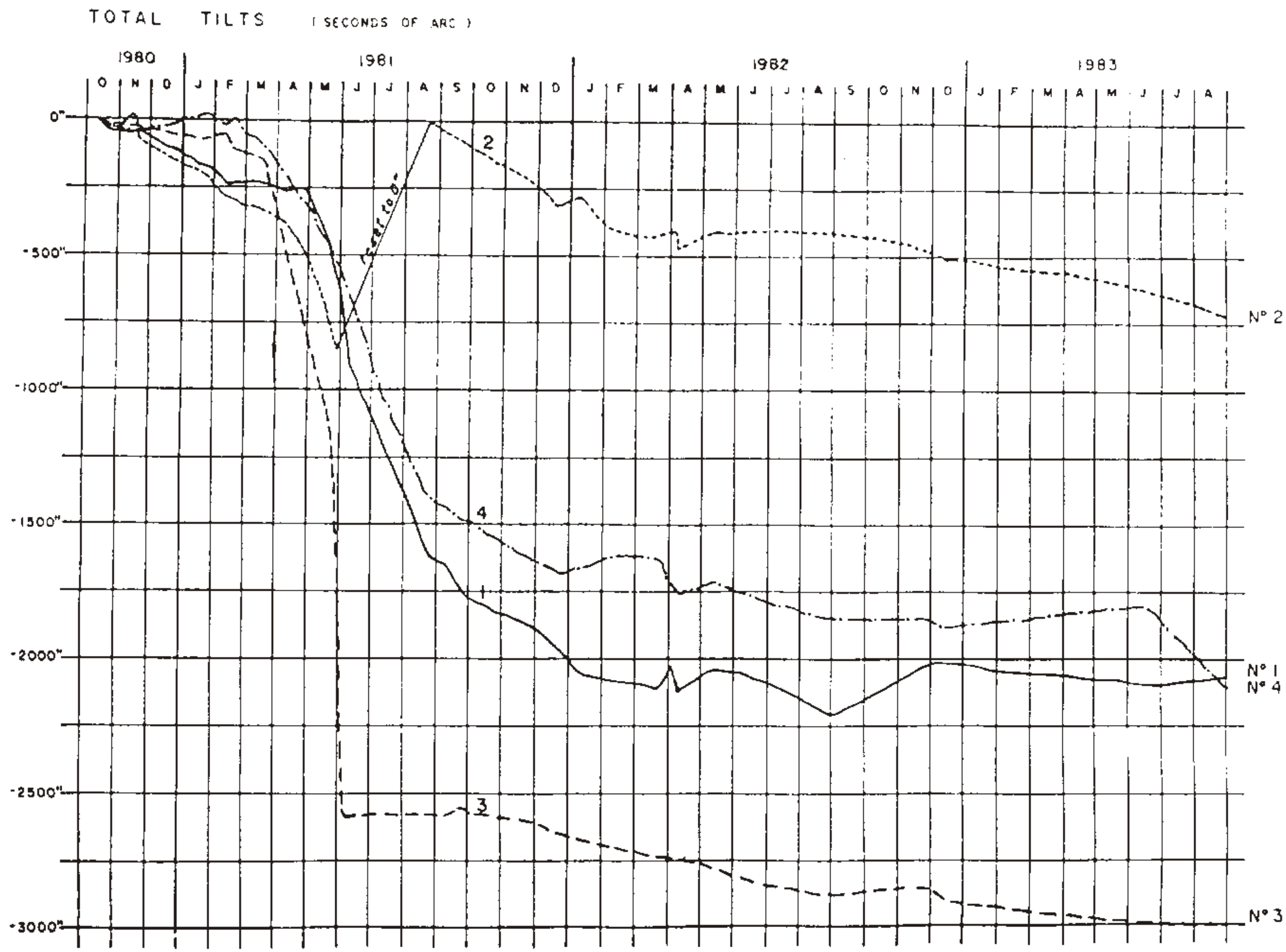

Fig. 2. Record of total tilts.

TABLE 1

Approximate coordinates of monitoring stations and observed displacements and tilts

Approximate station coordinates (m)				Displacement components and their standard deviations (m)					
Station	X/E	Y/N	Z/H	DX	σ	DY	σ	DZ	σ
Geodetic observations									
1	0.000	0.000	1901.920	−0.870	0.080	−0.100	0.080	−0.890	0.150
2	−47.760	−40.240	1861.940	−0.950	0.080	−0.170	0.080	−0.910	0.150
4	−142.620	−147.940	1753.540	−1.370	0.080	−0.470	0.080	−1.310	0.150
5	−244.750	−211.150	1674.260	−1.410	0.080	−0.380	0.080	−1.730	0.150
A1	−73.220	116.730	1903.540	−1.420	0.080	−0.190	0.080	−1.600	0.150
A2	−119.220	71.910	1862.010	−1.610	0.080	−0.420	0.080	−1.770	0.150
A3	−195.730	−9.490	1777.020	−1.660	0.080	−0.450	0.080	−1.950	0.150
A4	−263.620	−85.250	1710.840	−1.440	0.080	−0.690	0.080	−1.550	0.150
B1	−119.340	72.010	1862.120	−1.510	0.080	−0.510	0.080	−1.760	0.150
B4	−330.820	104.730	1710.060	−1.960	0.080	−0.670	0.080	−2.180	0.150
T0	−14.840	57.670	1916.560	−1.230	0.080	−0.150	0.080	−1.080	0.150
T1	45.880	47.220	1935.960	1.120	0.080	−0.050	0.080	−0.810	0.150
T2	−98.870	96.450	1889.110	−1.760	0.080	−0.460	0.080	−1.570	0.150
T3	−124.110	204.540	1887.890	−1.720	0.080	−0.460	0.080	−1.420	0.150
T4	−52.200	−22.400	1864.160	−1.070	0.080	−0.250	0.080	−0.990	0.150
Photogrammetric observations									
P1	−143.084	200.778	1872.913	−2.250	0.200	−0.380	0.200	−1.040	0.300
P2	−175.244	197.658	1851.179	−2.040	0.200	−0.610	0.200	−1.960	0.300
P3	−198.635	187.084	1831.305	−1.660	0.200	−0.460	0.200	−1.790	0.300
P4	−228.126	170.168	1804.028	−0.880	0.200	−1.270	0.200	−1.000	0.300
P5	−260.037	169.388	1784.374	−1.800	0.200	−0.690	0.200	−1.500	0.300

P6	−253.790	128.100	1769.042	−1.973	0.200	−0.700	0.200	−1.750	0.300
P7	−299.973	160.122	1753.901	−2.314	0.200	−0.980	0.200	−2.260	0.300
P8	−110.944	174.329	1888.986	−1.461	0.200	−0.410	0.200	−1.110	0.300
P9	−109.852	77.759	1869.673	−1.360	0.200	−0.567	0.200	−1.650	0.300
P10	−136.990	44.722	1832.980	−1.730	0.200	−0.350	0.200	−1.610	0.300
P11	−151.492	36.411	1821.794	−1.820	0.200	−0.520	0.200	−2.450	0.300
P12	−169.429	16.839	1801.775	−2.010	0.200	−0.160	0.200	−2.140	0.300
P13	−213.256	−9.299	1770.241	−1.820	0.200	−0.620	0.200	−1.580	0.300
P14	−263.210	−20.368	1747.964	−1.940	0.200	−0.680	0.200	−2.090	0.300
P15	−298.213	−43.793	1716.924	−1.240	0.200	−1.440	0.200	−1.510	0.300
P17	−49.878	−57.124	1849.808	−1.040	0.200	−0.280	0.200	−0.930	0.300
P18	−124.962	−15.079	1810.664	−1.700	0.200	−0.540	0.200	−1.410	0.300
P19	−147.402	−34.829	1788.645	−1.320	0.200	−0.590	0.200	−1.020	0.300
P21	−273.264	−94.973	1699.696	−0.990	0.200	−0.510	0.200	−1.580	0.300
P22	−23.818	−16.468	1881.710	−1.210	0.200	−0.090	0.200	−1.150	0.300
P23	−19.881	12.894	1895.275	−1.840	0.200	−0.128	0.200	−1.510	0.300
P24	−16.504	44.058	1910.460	−1.340	0.200	−0.300	0.200	−0.780	0.300
P29	−177.990	−150.611	1735.831	−1.710	0.200	−0.520	0.200	−0.680	0.300
P30	−211.152	−183.955	1704.884	−1.580	0.200	−0.430	0.200	−1.000	0.300
P31	−299.143	−225.496	1640.257	−1.350	0.200	−0.760	0.200	−1.600	0.300
P34	−112.577	231.708	1879.399	−1.190	0.200	−0.130	0.200	−1.020	0.300
P36	−69.030	111.562	1901.571	−1.050	0.200	−0.200	0.200	−1.950	0.300
P38	−38.803	129.198	1910.744	−1.360	0.200	−0.070	0.200	−1.000	0.300
P39	42.925	75.902	1940.332	−1.160	0.200	−0.040	0.200	−0.780	0.300

Observed tilts (arcsec)

	Tx		*Ty*	
T1	2077.000	30.000	−754.000	30.000
T3	2588.000	30.000	1248.000	30.000
T4	1474.000	30.000	−1105.000	30.000

For the two components τ_x and τ_y of the tilt observations at a point i:

$$\tau_x = \frac{\partial}{\partial x} w(x_i, y_i) \tag{7a}$$

$$\tau_y = \frac{\partial}{\partial y} w(x_i, y_i) \tag{7b}$$

Following the steps of the generalized approach, several possible deformation models were fitted to the observations and statistically tested. The following displacement function was finally accepted as the "best" model:

$$u(x, y) = a_0 + a_1 x + a_2 y + a_3 xy + a_6 x^2 y + a_8 x^3 + a_9 y^3 \tag{8a}$$

$$v(x, y) = b_0 + b_2 y + b_3 xy + b_4 x^2 + b_6 x^2 y + b_8 x^3 \tag{8b}$$

$$w(x, y) = c_0 + c_1 x + c_2 y + c_3 xy + c_4 x^2 + c_5 y^2 + c_6 x^2 y + c_7 xy^2 + c_8 x^3 \tag{8c}$$

Table 2 lists the estimated coefficients and their $(1-\alpha)$ significances together with the global test of the model. As one can see from the results, all the coefficients are significant at probabilities higher than 87% [$(1-\alpha) > 0.87$]. The significance of 1.000 in the computer output was printed for $(1-\alpha) > 0.999$. The global test passed. Figure 3 shows a computer-generated graphical display of the ground subsidence calculated from the model.

In this particular example, a similar subsidence model would have been obtained when using only geodetic and photogrammetric data without the three tilt stations. However, the continuous record of the tilts supplied important information on some

TABLE 2

Coefficients of the deformation model and their $(1-\alpha)$ significances

	Coefficients	$(1-\alpha)$		Coefficients	$(1-\alpha)$
A0	0.9158274408D 00	1.0000	B4	−0.1792043467D-04	0.9999
B0	−0.1858565290D 00	1.0000	B6	0.4364056549D-07	0.8767
C0	−0.9706251681D 00	1.0000	B8	−0.4143482424D-07	0.9943
A1	0.5136725012D-02	1.0000	C1	0.9933722003D-02	1.0000
A2	−0.5128189933D-02	1.0000	C2	−0.6688397490D-02	1.0000
A3	−0.3832308799D-04	0.9975	C3	−0.7137434691D-04	1.0000
A6	−0.1184677505D-06	0.9994	C4	0.3884618663D-04	1.0000
A8	−0.3213389714D-07	1.0000	C5	0.5845810260D-04	1.0000
A9	0.3894232203D-07	0.9948	C6	−0.2332744889D-06	1.0000
B2	0.1523455053D-02	0.9247	C7	0.3245244405D-06	1.0000
B3	0.1997947764D-04	0.9514	C8	0.2888329518D-07	1.0000

Estimated variance factor: 1.2382997605

Degrees of freedom: 102

Chi squared test at 0.05: $0.9580 < 1.0 < 1.6632$?

Chi squared test at 0.01: $0.8860 < 1.0 < 1.8321$?

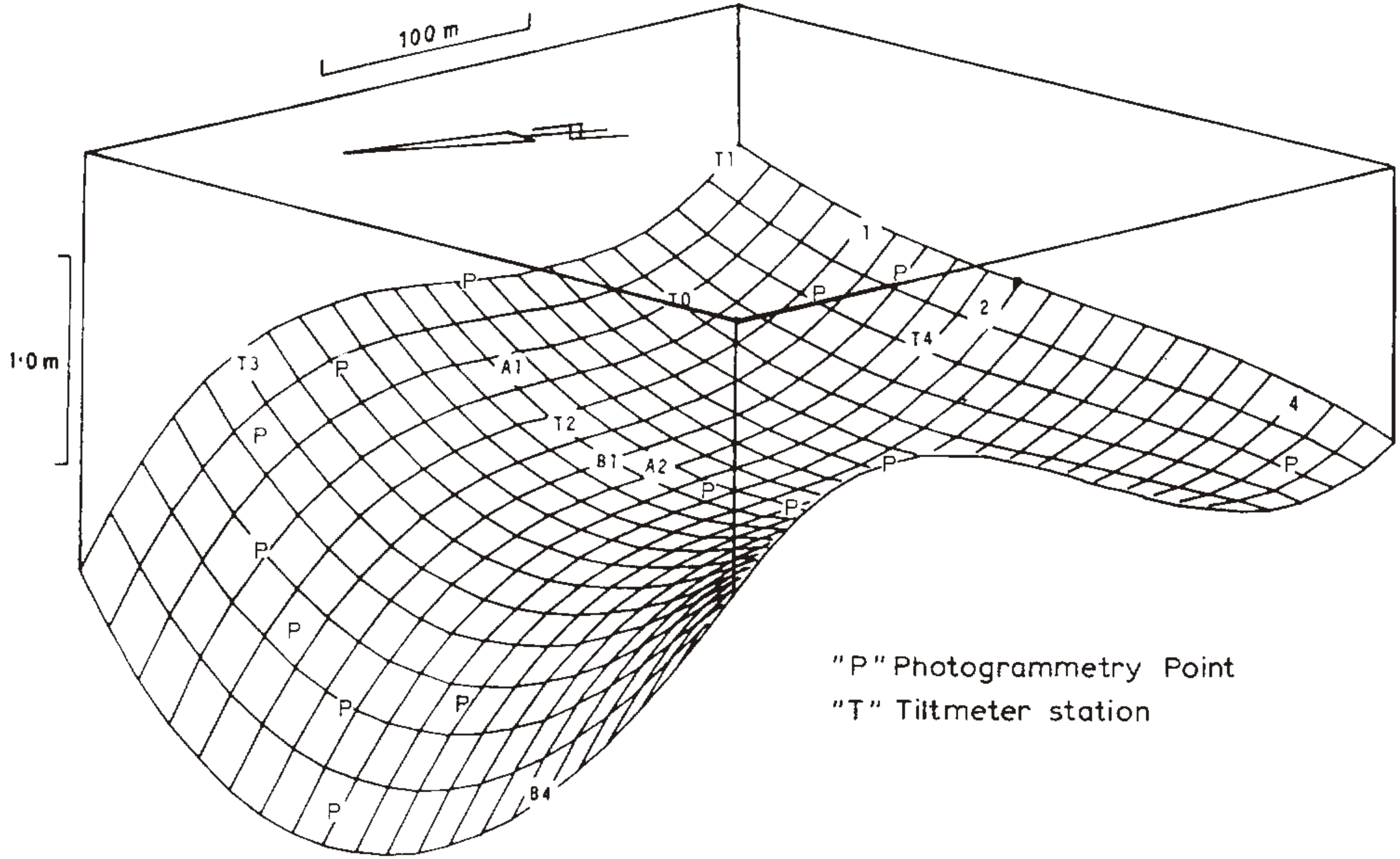

Fig. 3. Graphical display of the subsidence.

abrupt changes in the movements of rock masses which can be seen on the display in Fig. 2 and which would have not been noticed without those observations. Detailed discussion on the subsidence interpretation in this example has been considered as being beyond the scope of this paper.

4. CONCLUSIONS

Integration of different types of observables is very important for a proper physical interpretation and better understanding of the deformation phenomena. In the geosciences, when the deformation studies extend over large areas, for instance, in investigation of earth crustal movements, an integration of space surveying techniques (e.g., GPS, VLBI) with micro-measurements (micro-geodetic and geotechnical) of the stability of the observing stations should be made. The generalized approach provides a tool for such analysis.

The example of the ground subsidence study in which the 3-D geodetic, photogrammetric, and tilt measurements have been integrated in the geometrical analysis demonstrates the flexibility of the approach.

Appendix I: THE FUNCTIONAL RELATIONSHIP BETWEEN DEFORMATION PARAMETERS AND OBSERVED QUANTITIES

(1) Observation of coordinates of point i, for instance, the coordinates derived from photogrammetric measurements or obtained using space techniques:

$$\begin{pmatrix} x_i(t) \\ y_i(t) \\ z_i(t) \end{pmatrix} = \begin{pmatrix} x_i(t_0) \\ y_i(t_0) \\ z_i(t_0) \end{pmatrix} + \begin{pmatrix} u_i \\ v_i \\ w_i \end{pmatrix} \tag{I-1}$$

or:

$$\boldsymbol{r}_i(t) = \boldsymbol{r}_i(t) + \boldsymbol{d}_i = \boldsymbol{r}_i(t_0) + \boldsymbol{B} \cdot \boldsymbol{c} \tag{I-1'}$$

where $\boldsymbol{r}_i$ is the position vector of point i, the others are defined in eqn. (1).

(2) Observation of coordinate difference between points i and j, e.g., levelling (height difference) observation, pendulum (displacement) observation.

$$\begin{pmatrix} x_j(t) - x_i(t) \\ y_j(t) - y_i(t) \\ z_j(t) - z_i(t) \end{pmatrix} = \begin{pmatrix} x_j(t_0) - x_i(t_0) \\ y_j(t_0) - y_i(t_0) \\ z_j(t_0) - z_i(t_0) \end{pmatrix} + \begin{pmatrix} u_j - u_i \\ v_j - v_i \\ w_j - w_i \end{pmatrix} \tag{I-2}$$

or:

$$\boldsymbol{r}_j(t) - \boldsymbol{r}_i(t_0) = \boldsymbol{r}_j(t_0) - \boldsymbol{r}_i(t_0) + \left\{ \boldsymbol{B}(x_j, y_j, z_j; t - t_0) - \boldsymbol{B}(x_i, y_i, z_i; t - t_0) \right\} \cdot \boldsymbol{c} \tag{I-2'}$$

(3) Observation of azimuth from point i to point j:

$$\alpha_{ij}(t)=\alpha_{ij}(t_0)+\left(-\frac{\cos\alpha_{ij}}{S_{ij}\cos\beta_{ij}},\frac{\sin\alpha_{ij}}{S_{ij}\cos\beta_{ij}}\right)\cdot\begin{pmatrix}u_j-u_i\\ v_j-v_i\end{pmatrix}\tag{I-3}$$

where β_{ij} and S_{ij} are the vertical angle and spatial distance from point i to point j, respectively.

The observation of a horizontal angle is expressed as the difference of two azimuths.

(4) Observation of the distance between point i and point j:

$$S_{ij}(t)=S_{ij}(t_0)+(\cos\beta_{ij}\sin\alpha_{ij},\cos\beta_{ij}\cos\alpha_{ij},\sin\beta_{ij})\cdot\begin{pmatrix}u_j-u_i\\ v_j-v_i\\ w_j-w_i\end{pmatrix}\tag{I-4}$$

(5) Observation of strain along the azimuth α and vertical angle β at point i:

$$\epsilon(t)=\epsilon(t_0)+\boldsymbol{P}^{\mathrm{T}}\boldsymbol{E}\boldsymbol{P}\tag{I-5}$$

where $\boldsymbol{P}^{\mathrm{T}}=(\cos\beta\sin\alpha,\cos\beta\cos\alpha,\sin\beta)$ and:

$$\boldsymbol{E}=\begin{pmatrix}\frac{\partial u}{\partial x}&\frac{\partial u}{\partial y}&\frac{\partial u}{\partial z}\\ \frac{\partial v}{\partial x}&\frac{\partial v}{\partial y}&\frac{\partial v}{\partial z}\\ \frac{\partial w}{\partial x}&\frac{\partial w}{\partial y}&\frac{\partial w}{\partial z}\end{pmatrix}$$

(6) Observation of a vertical angle at point i to point j:

$$\beta_{ij}(t)=\beta_{ij}(t_0)+\left(-\frac{\sin\beta_{ij}\sin\alpha_{ij}}{S_{ij}},-\frac{\sin\beta_{ij}\cos\alpha_{ij}}{S_{ij}},\frac{\cos\beta_{ij}}{S_{ij}}\right)\cdot\begin{pmatrix}u_j-u_i\\ v_j-v_i\\ w_j-w_i\end{pmatrix}$$

(7) Observation of a horizontal tiltmeter:

$$\tau(t)=\tau(t_0)+\frac{\partial w}{\partial x}\sin\alpha+\frac{\partial w}{\partial y}\cos\alpha\tag{I-7}$$

where α is the orientation of the tiltmeter.

Appendix II: SOME TYPICAL DEFORMATION MODELS (Chrzanowski et al., 1982)

(1) *Single point displacement* or a *rigid body displacement* (Fig. 4a) of a group of points (say block B) with respect to a stable block (say block A); the deformation model is:

$$u_A(x,y)=0,\ v_A(x,y)=0,\ u_B(x,y)=a_0\ \text{and}\ v_B(x,y)=b_0\tag{II-1}$$

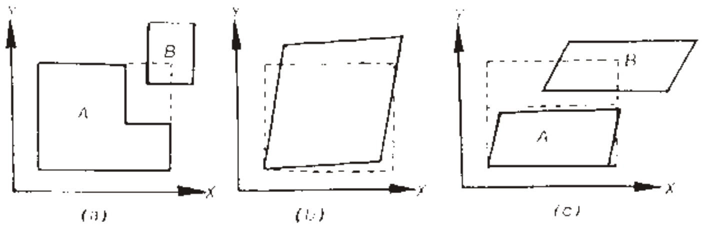

Fig. 4. Typical deformation models.

(2) *Homogeneous strain* (Fig. 4b) in the whole body without discontinuities; for the whole body, the linear deformation model is:

$$u(x, y) = a_1 x + a_2 y \text{ and } v(x, y) = b_1 x + b_2 y \tag{II-2}$$

which, after using the well-known infinitesimal strain displacement relationships, becomes:

$$u(x, y) = \epsilon_x \cdot x + \epsilon_{xy} \cdot y - \omega y \tag{II-3}$$

$$v(x, y) = \epsilon_{xy} \cdot x + \epsilon_y \cdot y + \omega x \tag{II-4}$$

where:

$$\epsilon_x = \frac{\partial u}{\partial x}, \quad \epsilon_y = \frac{\partial v}{\partial y}, \quad \epsilon_{xy} = \tfrac{1}{2}\left(\frac{\partial v}{\partial x} + \frac{\partial u}{\partial y}\right)$$

and:

$$\omega = \tfrac{1}{2}\left(\frac{\partial v}{\partial x} - \frac{\partial u}{\partial y}\right)$$

(3) A deformable body with one discontinuity, say between blocks A and B, with different linear deformations of each block plus a rigid body displacement of B with respect to A (Fig. 4c):

$$u_A(x, y) = a_1 x + a_2 y \tag{II-5}$$

$$v_A(x, y) = b_1 x + b_2 y \tag{II-6}$$

$$u_B(x, y) = c_0 + c_1 x + c_2 y \tag{II-7}$$

$$v_B(x, y) = g_0 + g_1 x + g_2 y \tag{II-8}$$

In the above case, components Δu_i and Δv_i of a total relative dislocation at any point i located on the discontinuity line between blocks A and B may be calculated as:

$$\Delta u_i = u_B(x_i, y_i) - u_A(x_i, y_i) \tag{II-9}$$

and:

$$\Delta v_i = v_B(x_i, y_i) - v_A(x_i, y_i) \tag{II-10}$$

Usually, the actual deformation model is a combination of the above simple models or, if more complicated, it is expressed by non-linear displacement functions which require fitting of higher order polynomials or other suitable functions.

If time-dependent deformation parameters are sought then the above deformation models will contain a time variable. For instance, in the first model above, if the velocity (rate) and acceleration of the dislocation of block B in respect to block A are to be found, the deformation model would be:

$$u_A = 0,\ v_A = 0,\ u_B = \dot{a}_0 t + \ddot{a}_0 t^2 \text{ and } v_B = \dot{b}_0 t + \ddot{b}_0 t^2 \tag{II-11}$$

and, in the model of the homogeneous strain, if a linear time dependence is assumed, the model becomes:

$$u(x,\ y,\ t) = \dot{\epsilon}_x xt + \dot{\epsilon}_{xy} yt - \dot{\omega} yt \tag{II-12}$$

$$v(x,\ y,\ t) = \dot{\epsilon}_{xy} xt + \dot{\epsilon}_y yt + \dot{\omega} xt \tag{II-13}$$

where the dot above the parameters indicates their rate (velocity) and the double dot, acceleration.

REFERENCES

Armenakis, C. and Faig, W. 1982. Subsidence monitoring by photogrammetry. Proc. 4th Can. Symp. on Mining Surveying and Deformation Measurements, Banff, pp. 197–208.

Chen, Y.Q., 1983. Analysis of Deformation Surveys—A Generalized Method. Dep. Surv. Eng. Tech. Rep. 94, Univ. New Brunswick, Fredericton, N.B.

Chrzanowski, A. and Fisekci, M.Y., 1982. Application of tiltmeters with a remote data acquisition in monitoring mining subsidence. Proc. 4th Can. Symp. on Mining Surveying and Deformation Surveys, Banff, pp. 321–333.

Chrzanowski, A., Faig, W., Kurz, B.J. and Makosinski, A., 1980. Development, installation and operation of a subsidence monitoring and telemetry system. Final report to the Canada Centre for Mineral and Energy Technology, Calgary.

Chrzanowski, A., Chen, Y.Q. and Secord, J.M., 1983. On the strain analysis of tectonic movements using fault-crossing micro-geodetic surveys. Tectonophysics, 97: 297–315.

Fisekci, M.Y. and Chrzanowski, A., 1981. Some aspects of subsidence monitoring in difficult terrain and climate conditions of Rocky Mountains, western Canada. In: S. Peng (Editor), Proc. Workshop on Surface Subsidence due to Underground Mining, Morgantown, WV, University of West Virginia, pp. 182–197.

Secord, J.M., 1984. Implementation of a generalized method for the analysis of deformation surveys. M.Sc.E. thesis, Department of Surveying Engineering, University of New Brunswick, Fredericton, N.B.

Sokolnikoff, I.S., 1956. Mathematical Theory of Elasticity. McGraw-Hill, New York.